

# Technical Report: Trajectory Optimization for Differential Drive Mobile Manipulators via Topological Paths Search and Arc Length-Yaw Parameterization

Long Xu<sup>†,1,2</sup>, Choilam Wong<sup>†,2</sup>, Mengke Zhang<sup>1,2</sup>, Junxiao Lin<sup>1,2</sup> and Fei Gao<sup>1,2</sup>

† Equal contribution

<sup>1</sup>Institute of Cyber-Systems and Control,  
College of Control Science and Engineering,  
Zhejiang University, Hangzhou 310027, China.

<sup>2</sup>Huzhou Institute of Zhejiang University, Huzhou 313000, China.

Corresponding author: Fei Gao Email: fgaoaa@zju.edu.cn

## Abstract

**We present an efficient hierarchical motion planning pipeline for differential drive mobile manipulators. Our approach first searches for multiple collision-free and topologically distinct paths for the mobile base to extract the space in which optimal solutions may exist. Further sampling and optimization are then conducted in parallel to explore feasible whole-body trajectories. For trajectory optimization, we employ polynomial trajectories and arc length-yaw parameterization, enabling efficient handling of the nonholonomic dynamics while ensuring optimality.**

## Introduction

Mobile manipulator, comprising a multi-joint manipulator mounted on a floating base, integrates precise environmental interaction ability of a manipulator arm and mobility of a wheeled robots. This synergistic combination has attracted significant attention in both industry and academia. As with other robots, autonomous navigation and obstacle avoidance are critical to enable mobile manipulators to perform a variety of tasks. The extra degrees of freedom that comes with the manipulator renders motion planning significantly more difficult, as safety must now be considered in a complex 3D space, instead of 2D space for wheeled robots. The enormous growth of the configuration space makes exploration substantially more demanding. The potential nonholonomic constraints of the chassis also impose additional challenges to the problem.

Intuitively, the presence of the manipulator only makes the robot more likely to collide with obstacles. In other words, the chassis paths of feasible mobile manipulator paths is a subset of the feasible paths for the chassis alone. Leveraging this fact, we shrink the configuration space for searching whole-body path substantially by conditioning it on 2D mobile base path. To ensure optimality and efficiency, we use multiple non-homotopic paths and employ parallel processing for each path. The efficacy of this approach is demonstrated in simulated experiments.

Polynomial trajectories have shown great efficiency in robot motion planning in recent years due to their smoothness and lower dimensionality compared to finite elements (1–4). Motivated by this, we use polynomials to represent the trajectory of a mobile manipulator, modeling the motion planning task as a trajectory optimization problem which can be solved efficiently to obtain safe, dynamically feasible trajectories for the robot. In this paper, we adopt arc length-yaw parameterization to tackle the nonholonomic constraints brought about by the mobile base.

This approach have been shown to be more efficient with comparison to other methods (2, 5).

The main contributions of this paper can be summarized as follows:

- We introduce topological path search in mobile base planning for mobile manipulators to efficiently extract the space in which optimal trajectories may lie.
- We take advantage of the efficiency of polynomial representations and propose a spatial-temporal trajectory optimization model for mobile manipulators, handling nonholonomic kinematics of the differential drive mobile base with arc length-yaw parameterizations.
- Integrating the above two modules, we propose an efficient optimization-based trajectory planning framework for differential drive mobile manipulators. Simulation experiments in complex environments verify the efficiency of our algorithm.

## **Related Works**

### **Sampling-based Motion Planning**

Sampling-based motion planning (SBMP) approximates the configuration space by sampling discrete waypoints uniformly or via heuristics-guided strategies (6). It incrementally constructs a graph, where nodes represent sampled waypoints and edges denote collision-free paths (typically determined through interpolation). A feasible path can then be derived by querying this graph. This approach is adopted by representative works, such as RRT\* (7), PRM\* (8), FMT\* (9), etc. SBMP typically provides two key theoretical guarantees: probabilistic completeness and asymptotic optimality. However, the performance of SBMP severely degrades in high-DoF systems, such as a mobile manipulator. The exponential growth of sampling space volume with dimensionality results in excessively long planning time in challenging scenarios (e.g. narrow passages), limiting the practicality of SBMP.

One approach to improve efficiency involves employing alternative sampling strategies informed by prior knowledge of the workspace. Since only a subset of sampled waypoints contribute to the final path, it is natural to prioritize sampling in regions where these waypoints are more likely to be found with regards to the workspace and the planning task i.e. using a biased sampling distribution conditioned on the workspace. (9) An advantage of this approach is its ability to preserve both guarantees of completeness and optimality by combining uniform distribution with the biased distribution. Leveraging this framework, numerous studies have proposed different sampling strategies. (10) synthesizes a sampler by querying a database built with past experience; (9, 11) use supervised learning to predict criticality or optimality of samples; (11, 12) use generative model to sample around optimal solution.

Alternative approach mitigates the performance degradation induced by high DoFs of mobile manipulator by decomposing the arm and base motions, one conditioned on another. Works adopting this approach, including REMANI (13) (to initialize optimization) and (14), enable SBMP applications on mobile manipulators, improving the efficiency of planning. However, the limitation is obvious, it sacrifices both completeness and asymptotic optimality, resulting in suboptimal paths.

## **Optimization-based Motion Planning**

Optimization-based motion planning (OBMP) represents another major approach. As surveyed by (15), these methods excel at incorporating robot dynamics and potential task-related constraints naturally, which SBMP can only achieve with considerable efficiency trade-offs. Several influential works have demonstrated these advantages, including CHOMP (16), STOMP (17), GPMP (18), etc. However, these capabilities come with fundamental limitations: OBMP is sensitive to initial values, offers no completeness guarantees, and may converge to local optima.

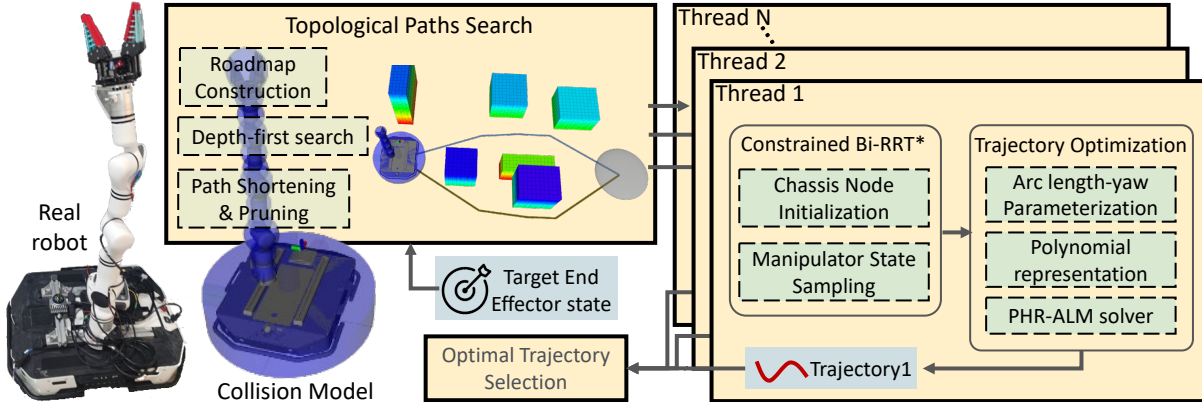


**Fig. 1.** Planning framework.

## Trajectory Planning Pipeline

Fig. 1 illustrates our planning framework. When the robot receives the target  $SE(3)$  pose of the end effector, it performs a topological path search to obtain mobile base paths with distinct homotopy. The planner then initializes the sequence of mobile base states for these paths and samples the manipulator states to obtain whole-body paths of the robot in parallel, which are subsequently handed over to the trajectory optimizer to obtain dynamically feasible trajectories.

We refer to the method proposed in work (19) to construct a 2D topological roadmap and perform path searching, shortening and pruning. We then construct paths in  $SE(2)$  space by sampling mobile base states at fixed intervals on the acquired topological paths. Each path is considered as a initial value of the multilayer constrained RRT\*-connect (13), and is sampled to obtain the whole-body trajectory, which is used as the initial value for trajectory optimization. The candidate paths are processed in parallel for efficiency.

## Trajectory Representation

We use the arc length  $s(t)$ , yaw angle  $\theta(t)$  of the mobile base, and the joint angles  $q_k(t)$  of the manipulator to denote the trajectory of the differential drive mobile manipulators, where  $k = 1, 2, \dots, N$  denote the indexes of the joints. Thus the  $SE(2)$  state of the mobile base is  $[x(t), y(t), \theta(t)]^T$ , where

$$x(t) = \int_0^t \dot{s}(\tau) \cos \theta(\tau) d\tau + x_0, \quad (1)$$

$$y(t) = \int_0^t \dot{s}(\tau) \sin \theta(\tau) d\tau + y_0, \quad (2)$$

$[x_0, y_0]^T$  is the initial position of the mobile base.

Following the optimality condition for multi-stage control effort minimization problem (1), we use quintic piecewise polynomials with four times continuously differentiable at the segmented points to represent the robot trajectories for minimizing jerk (20). Each piece of trajectory is denoted as:

$$s_j(t) = \mathbf{c}_{s_j}^T \gamma(t) \quad t \in [0, T_j], \quad (3)$$

$$\theta_j(t) = \mathbf{c}_{\theta_j}^T \gamma(t) \quad t \in [0, T_j], \quad (4)$$

$$q_{kj}(t) = \mathbf{c}_{q_{kj}}^T \gamma(t) \quad t \in [0, T_j], \quad (5)$$

where  $j = 1, 2, \dots, M$  is the index of piecewise polynomial,  $T_j$  is the duration of a piece of the trajectory,  $c_* \in \mathbb{R}^6$ ,  $* = \{s_j, \theta_j, q_{kj}\}$  is the coefficient of polynomial,  $\gamma(t) = [1, t, t^2, \dots, t^5]^T$  is the natural base. Following the work (2), we employ Simpson's rule to calculate the integrals (1) and (2).

## Trajectory Optimization

In this paper, we formulate the trajectory optimization problem for differential drive mobile manipulators as:

$$\min_{\mathbf{c}, \mathbf{e}, \mathbf{T}} f(\mathbf{c}, \mathbf{e}, \mathbf{T}) = \int_0^{\sum_{j=1}^M T_j} \mathbf{j}(t)^T \mathbf{W} \mathbf{j}(t) dt + \rho \|\mathbf{T}\|_1 \quad (6)$$

$$s.t. \quad \mathbf{FK}(\mathbf{e}_f) = \mathbf{p}_e, \quad (7)$$

$$\mathbf{M}(\mathbf{T})\mathbf{c} = \mathbf{b}(\mathbf{P}, \mathbf{e}), \quad \mathbf{T} > \mathbf{0}, \quad (8)$$

$$|v_{\max}\omega(t) \pm \omega_{\max}v(t)| \leq v_{\max}\omega_{\max}, \quad (9)$$

$$a^2(t) \leq a_{\max}^2, \quad \beta^2(t) \leq \beta_{\max}^2, \quad (10)$$

$$(\mathbf{q} \circ \mathbf{q})(t) \leq \mathbf{q}_{\max 2}, \quad (\dot{\mathbf{q}} \circ \dot{\mathbf{q}})(t) \leq \dot{\mathbf{q}}_{\max 2}, \quad (11)$$

$$(\ddot{\mathbf{q}} \circ \ddot{\mathbf{q}})(t) \leq \ddot{\mathbf{q}}_{\max 2}, \quad (12)$$

$$\mathbf{SDF}(\mathbf{ColliPts}(\mathbf{c}, \mathbf{T})) \geq \mathbf{r}_{thr}, \quad (13)$$

$$\mathbf{SelfColli}(\mathbf{c}, \mathbf{T}) \geq \mathbf{0}, \quad (14)$$

where  $\mathbf{c} = [\mathbf{c}_1^T, \mathbf{c}_2^T, \dots, \mathbf{c}_M^T]^T \in \mathbb{R}^{6M \times (N+2)}$ ,  $\mathbf{c}_k = [\mathbf{c}_{k1}, \mathbf{c}_{k2}, \dots, \mathbf{c}_{k(N+2)}] \in \mathbb{R}^{6 \times (N+2)}$ ,  $k = 1, 2, \dots, M$  are coefficient matrices. For other optimization variables,  $\mathbf{e}_f = [x_f, y_f, \theta_f, \mathbf{q}_f]^T$ ,  $\mathbf{T} = [T_1, T_2, \dots, T_M]^T$  denote the end state of the robot and time durations of the trajectory, respectively, where  $\mathbf{q}_f = [q_{1f}, q_{2f}, \dots, q_{Nf}]$ .  $x_f, y_f$  are calculated using  $\mathbf{e} = [s_f, \theta_f, \mathbf{q}]^T$  and  $\mathbf{c}, \mathbf{T}$ .

In the objective function  $f(\mathbf{c}, \mathbf{e}, \mathbf{T})$ ,  $\mathbf{j}(t) = [s^{(3)}(t), \theta^{(3)}(t), \mathbf{q}^{(3)}(t)]^T$  denote the jerk of the trajectory.  $\mathbf{W} \in \mathbb{R}^{(2+N) \times (2+N)}$  is diagonal positive matrix representing the weights.  $\rho > 0$  is a constant to give the trajectory some aggressiveness.

Eq.(7) denotes the end-effector pose constraints for the robot end state.  $\mathbf{FK} : SE(2) \times \mathbb{R}^N \mapsto SE(3)$  is the forward kinematics function. Conditions (8) denotes the combinations of the

continuity constraints mentioned in last subsection and boundary conditions of the trajectory:

$$[s(0), \dot{s}(0), \ddot{s}(0)] = [0, v_0, a_0], \quad (15)$$

$$[\theta(0), \dot{\theta}(0), \ddot{\theta}(0)] = [\theta_0, \omega_0, \beta_0], \quad (16)$$

$$[\mathbf{q}(0), \dot{\mathbf{q}}(0), \ddot{\mathbf{q}}(0)] = [\mathbf{q}_0, \dot{\mathbf{q}}_0, \ddot{\mathbf{q}}_0], \quad (17)$$

$$[s(T_f), \dot{s}(T_f), \ddot{s}(T_f)] = [s_f, 0, 0], \quad (18)$$

$$[\theta(T_f), \dot{\theta}(T_f), \ddot{\theta}(T_f)] = [\theta_f, 0, 0], \quad (19)$$

$$[\mathbf{q}(T_f), \dot{\mathbf{q}}(T_f), \ddot{\mathbf{q}}(T_f)] = [\mathbf{q}_f, \mathbf{0}, \mathbf{0}]. \quad (20)$$

$\mathbf{P} \in \mathbb{R}^{(N+2) \times (M-1)}$  is the segment points matrix of the trajectories.  $T_f = \|\mathbf{T}\|_1$  denote the total duration of the trajectory.

Conditions (9)~(12) are dynamic feasibility constraints, including coupled linear velocity and angular velocity constraints (2), limitation of linear acceleration  $a(t) = \dot{s}(t)$ , angular acceleration  $\beta(t) = \dot{\omega}(t)$ , joint angles, joint angular velocities and joint angular accelerations, where  $v_{\max}, \omega_{\max}, a_{\max}, \beta_{\max}, \mathbf{q}_{\max 2}, \dot{\mathbf{q}}_{\max 2}, \ddot{\mathbf{q}}_{\max 2}$  are constants.

Condition (13) denotes obstacle avoidance constraints related to the environment. In this paper, we construct a Signed Distance Field (SDF) to represent the environment. In SDF, the value at each state of the space is the distance to the edge of the nearest obstacle, where the value inside the obstacle is negative. As shown in the robot collision model in Fig. 1, we approximate the collision geometry using a set of cylinder and spheres. The function **ColliPts**( $\cdot$ ) maps the state points in the trajectory to collision detection point sets, i.e., the centers of the cylinder and the spheres. The function **SDF**( $\cdot$ ) maps the set of points to the corresponding SDF values, where the SDF of the center of the mobile base is constructed with a 2D grid map.  $\mathbf{r}_{thr}$  is a constant vector, which includes the radii of the cylinder and spheres. Condition (14) denotes obstacle avoidance constraints related to the robot itself. Since our collision model uses cylinder and spheres, the function **SelfColli**( $\cdot$ ) calculates the distance vector representing the distance

between each pair of them, corresponding to each state point of the trajectory.

## Problem Solving

We refer the work (1) to cope with Conditions (8), converting the optimization variables  $\{c, e, T\}$  to  $\{P, e, \tau\}$ . where for each element  $T_j$  in  $T$  and  $\tau_j$  in  $\tau$ , we have

$$\tau_j = L_{c2}(T_j) = \begin{cases} 1 - \sqrt{2T_j^{-1} - 1} & 0 < T_j \leq 1 \\ \sqrt{2T_j - 1} - 1 & T_j > 1 \end{cases}. \quad (21)$$

To guarantee that constraint  $(q \circ q)(t) \leq q_{\max 2}$  is satisfied when  $t = T_j, j = 1, 2, \dots, M$  and at  $q_f$ , we use the following inverse sigmoid-like function to convert  $q_f$  and each element of the submatrix  $Q \in \mathbb{R}^{6M \times N}$  of  $P$  with respect to the joint angles of the manipulator to  $q_f$  and  $Q_f$ , respectively:

$$q(q) = L_{c2} \left( \frac{q_{\max} + q}{q_{\max} - q} \right). \quad (22)$$

To deal with continuous polynomial trajectories, we discretize each piece of the duration  $T_j$  as  $K$  time stamps  $\tilde{t}_l = (l/K) \cdot T_j, l = 0, 1, \dots, K - 1$ , and impose the constraints on these time stamps. To efficiently solve this optimization problem, we convert all inequality constraints into penalty terms and add them to the objective function as discrete integrals. Specifically, let the objective function be  $f(\text{traj}(t))$ , and the constraint function be  $\mathcal{C}(\text{traj}(t))$ , then the new objective function is

$$f(\text{traj}(t)) + \rho_c \sum_{j=1}^M \sum_{l=0}^{K-1} \frac{T_j}{K} \mathcal{L}(\max\{0, \mathcal{C}[\text{traj}_j(\frac{lT_j}{K})]\}), \quad (23)$$

where  $\mathcal{L}$  denotes a function that smooths the constraint function  $\mathcal{C}$  into a  $C^2$  function,  $\text{traj}_j$  is the  $j$ -th polynomial trajectory.  $\rho_c$  denotes the penalty weight.

For Equation constraint (7), we use the continuous representation proposed in work (21) to map  $e_f \in SE(3)$  to  $e_c \in \mathbb{R}^9$ , then processing the constraint using Powell-Hestenes-Rockafellar Augmented Lagrangian method (22) (PHR-ALM). In this work, the efficient quasi-Newton optimizer L-BFGS (23) is chosen as the inner loop iteration algorithm for PHR-ALM.

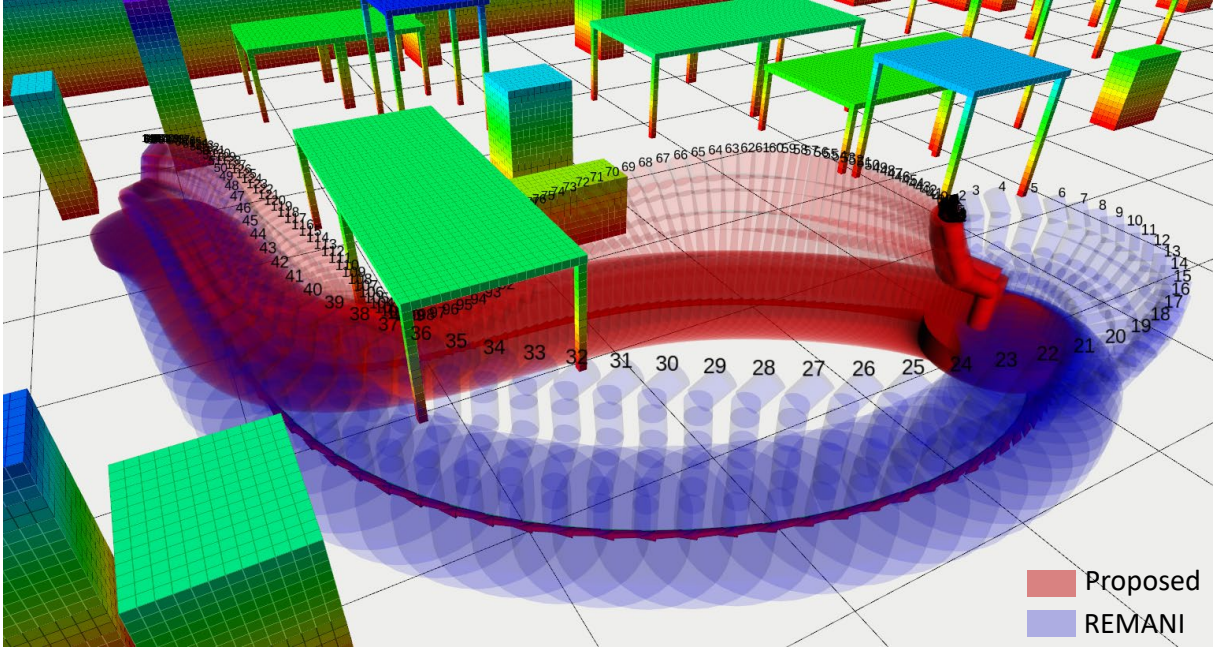


**Fig. 2.** Simulation experiments.

## Results

We compare REMANI (13) with proposed method in a simulation environment deployed on a local device (equipped with an Intel i7-12700). As shown in the Fig. 2, we randomly place variable sized obstacles resembling desks and cuboids in a  $35m \times 15m$  walled room to simulate an environment cluttered with obstacles. Specifically, there are 30 grids of desks, each grids consisting of one or two rows or columns of desks (of dimensions  $(0.75 \sim 1.25m) \times (0.75 \sim 1.25m) \times (0.5 \sim 1.5m)$ ) placed side by side, and 60 cuboids of dimensions  $(0.2 \sim 0.8m) \times (0.2 \sim 0.8m) \times (0.4 \sim 1.5m)$ . Additionally, each desk or cuboids are generated with rejection sampling to avoid overlapping and no cuboids are placed under desk.

Within this environment, we tested the two planners in three different distance intervals between the start and end mobile base positions ( $3 \sim 8m$ ,  $8 \sim 15m$ , and  $15 \sim 30m$ ). For each distance interval, we randomly generated 500 sets of collision-free start and target states

for the mobile manipulator, along with randomly generated obstacle positions and sizes. We then used both REMANI (13) and proposed method to generate trajectories between each set of start and target states, recording the average success rate (S.R.), average time consumption (T.P.) and average trajectory duration (T.D.). The results are shown in Table 1.

The planner will be considered failed if it cannot find a whole-body path to initialize trajectory optimization or the optimized trajectory does not satisfy the safety and dynamic constraints. For this experiment, REMANI searches for whole-body path by performing 3 trials with hybrid A\* and multilayer constrained RRT\*-Connect before 1 final attempt with whole-body search. The states are sampled from the front-end path at a time resolution of 1.0s for the initialization of the MINCO (1) trajectory.

Table 1: Algorithm Comparisons

Scale	Method	S.R. (%)	T.P. (ms)	T.D. (s)
Small (3m~8m)	REMANI (13)	62.4	318.9	13.8
	Proposed	92.0	107.7	13.2
Medium (8m~15m)	REMANI (13)	73.8	810.8	20.5
	Proposed	91.0	227.5	20.4
Large (15m~30m)	REMANI (13)	51.4	2799.8	32.9
	Proposed	79.8	522.2	32.0

The proposed method demonstrates significantly improved robustness, evidenced by the notably higher average success rate across all three distance intervals. We attribute this enhancement to the usage of topological paths and arc length-yaw parameterization. The former enables exploration of different possible solutions for further exploitation, while the latter theoretically solves the difficulty of constraining the angular velocity and angular acceleration of the mobile base due to the singularity brought about by differential flatness. (2, 3)

The results also indicate a significant advantage on efficiency of the proposed pipeline,

which consumes considerably lower planning time in all three distance intervals. The advantage on efficiency derive from the hierarchical planning strategy and extensive usage of parallel processing. Similar to REMANI (13), the hierarchical planning strategy effectively decompose the motion of the mobile base and the manipulator. The topological paths for the mobile base limit subsequent high DoF manipulator path searching to a substantially smaller configuration space. Meanwhile, the computationally expensive components of the pipeline, namely path searching of the manipulator and trajectory optimization, are conducted in parallel, enabling algorithm exploiting each of the topological paths efficiently, reducing the time consumption of planning to reach acceptable success rate.

## **Discussion**

In this paper, we propose a hierarchical planner for motion planning of differential drive mobile manipulators. Although this pipeline shows higher efficiency and success rate in complex scenarios compared to existing approaches, there are still cases of long-time consuming or even failure. Meanwhile, in such a classical framework, the environment is treated as non-interactive, which is in great contradiction with the powerful interactivity of the manipulators. Such a setting is tantamount to cutting off one's own arm. Neural networks, as a powerful implicit representation, have been shown to be a promising technique in motion planning (3, 24, 25). In the future, we will try to incorporate neural networks for more efficient algorithms.

## **Acknowledgments**

The project was funded by HUAWEI central research institute - application innovation lab.

## References

1. Z. Wang, X. Zhou, C. Xu, F. Gao, Geometrically constrained trajectory optimization for multicopters, *IEEE Transactions on Robotics* **38**, 3259–3278 (2022).
2. M. Zhang, N. Chen, H. Wang, J. Qiu, Z. Han, Q. Ren, C. Xu, F. Gao, Y. Cao, Universal trajectory optimization framework for differential drive robot class, *IEEE Transactions on Automation Science and Engineering* (2025).
3. Z. Han, M. Tian, Z. Gongye, D. Xue, J. Xing, Q. Wang, Y. Gao, J. Wang, C. Xu, F. Gao, Hierarchically depicting vehicle trajectory with stability in complex environments, *Science Robotics* **10**, eads4551 (2025).
4. Z. Han, Y. Wu, T. Li, L. Zhang, L. Pei, L. Xu, C. Li, C. Ma, C. Xu, S. Shen, *et al.*, An efficient spatial-temporal trajectory planner for autonomous vehicles in unstructured environments, *IEEE Transactions on Intelligent Transportation Systems* **25**, 1797–1814 (2023).
5. M. Zhang, C. Xu, F. Gao, Y. Cao, Trajectory optimization for 3d shape-changing robots with differential mobile base, *2023 IEEE International Conference on Robotics and Automation (ICRA)* (IEEE, 2023), pp. 10104–10110.
6. J. D. Gammell, S. S. Srinivasa, T. D. Barfoot, Informed rrt\*: Optimal sampling-based path planning focused via direct sampling of an admissible ellipsoidal heuristic, *2014 IEEE/RSJ international conference on intelligent robots and systems* (IEEE, 2014), pp. 2997–3004.
7. S. Karaman, E. Frazzoli, Sampling-based algorithms for optimal motion planning, *The international journal of robotics research* **30**, 846–894 (2011).

8. L. Janson, E. Schmerling, A. Clark, M. Pavone, Fast marching tree: A fast marching sampling-based method for optimal motion planning in many dimensions, *The International journal of robotics research* **34**, 883–921 (2015).
9. B. Ichter, E. Schmerling, T.-W. E. Lee, A. Faust, Learned critical probabilistic roadmaps for robotic motion planning, *2020 IEEE International Conference on Robotics and Automation (ICRA)* (IEEE, 2020), pp. 9535–9541.
10. C. Chamzas, A. Shrivastava, L. E. Kavraki, Using local experiences for global motion planning, *2019 International Conference on Robotics and Automation (ICRA)* (IEEE, 2019), pp. 8606–8612.
11. Y. Lu, Y. Ma, D. Hsu, P. Cai, Neural randomized planning for whole body robot motion, *arXiv preprint arXiv:2405.11317* (2024).
12. B. Ichter, J. Harrison, M. Pavone, Learning sampling distributions for robot motion planning, *2018 IEEE International Conference on Robotics and Automation (ICRA)* (IEEE, 2018), pp. 7087–7094.
13. C. Wu, R. Wang, M. Song, F. Gao, J. Mei, B. Zhou, Real-time whole-body motion planning for mobile manipulators using environment-adaptive search and spatial-temporal optimization, *2024 IEEE International Conference on Robotics and Automation (ICRA)* (IEEE, 2024), pp. 1369–1375.
14. S. Chitta, B. Cohen, M. Likhachev, Planning for autonomous door opening with a mobile manipulator, *2010 IEEE International Conference on Robotics and Automation* (IEEE, 2010), pp. 1799–1806.

15. Z. Zhao, S. Cheng, Y. Ding, Z. Zhou, S. Zhang, D. Xu, Y. Zhao, A survey of optimization-based task and motion planning: From classical to learning approaches, *IEEE/ASME Transactions on Mechatronics* (2024).
16. M. Zucker, N. Ratliff, A. D. Dragan, M. Pivtoraiko, M. Klingensmith, C. M. Dellin, J. A. Bagnell, S. S. Srinivasa, Chomp: Covariant hamiltonian optimization for motion planning, *The International journal of robotics research* **32**, 1164–1193 (2013).
17. M. Kalakrishnan, S. Chitta, E. Theodorou, P. Pastor, S. Schaal, Stomp: Stochastic trajectory optimization for motion planning, *2011 IEEE international conference on robotics and automation* (IEEE, 2011), pp. 4569–4574.
18. M. Mukadam, X. Yan, B. Boots, Gaussian process motion planning, *2016 IEEE international conference on robotics and automation (ICRA)* (IEEE, 2016), pp. 9–15.
19. B. Zhou, F. Gao, J. Pan, S. Shen, Robust real-time uav replanning using guided gradient-based optimization and topological paths, *2020 IEEE International Conference on Robotics and Automation (ICRA)* (IEEE, 2020), pp. 1208–1214.
20. B. Sundaralingam, S. K. S. Hari, A. Fishman, C. Garrett, K. Van Wyk, V. Blukis, A. Mil-lane, H. Oleynikova, A. Handa, F. Ramos, *et al.*, curobo: Parallelized collision-free minimum-jerk robot motion generation, *arXiv preprint arXiv:2310.17274* (2023).
21. Y. Zhou, C. Barnes, J. Lu, J. Yang, H. Li, On the continuity of rotation representations in neural networks, *Proceedings of the IEEE/CVF conference on computer vision and pattern recognition* (2019), pp. 5745–5753.
22. R. T. Rockafellar, Augmented lagrange multiplier functions and duality in nonconvex programming, *SIAM Journal on Control* **12**, 268–285 (1974).

23. D. C. Liu, J. Nocedal, On the limited memory bfgs method for large scale optimization, *Mathematical programming* **45**, 503–528 (1989).
24. S. Yan, Z. Zhang, M. Han, Z. Wang, Q. Xie, Z. Li, Z. Li, H. Liu, X. Wang, S.-C. Zhu, M 2 diffuser: Diffusion-based trajectory optimization for mobile manipulation in 3d scenes, *IEEE Transactions on Pattern Analysis and Machine Intelligence* (2025).
25. T. Yang, J. Hwang, J. Jeong, M. Yoon, S.-E. Yoon, Efficient navigation among movable obstacles using a mobile manipulator via hierarchical policy learning, *arXiv preprint arXiv:2506.15380* (2025).